

An aberration-free lens with zero F-number

D. Schurig

North Carolina State University, Department of ECE,
Campus Box 7911, Raleigh, NC, 27695

Abstract: Starting from the Luneberg lens index profile, we apply the transformation design method to the problem of far-field imaging of (infinitely) distant objects. This analysis yields a single element lens with a planar image surface, zero aberrations of all orders, zero F-number and (in some cases) constant aperture for all angles of incidence.

1 Introduction

Transformation design – the use of coordinate transforms to design material objects – has proven useful for obtaining specifications that will implement interesting and useful electromagnetic and acoustic devices. As the required material specifications can be quite complex it would be difficult to find them by other means. However, with transformation design, once the technique is understood, one can proceed directly (albeit carefully) from concept to material specification. Specifications for invisibility cloaks[1, 2, 3], near-field focusing devices[4], beam steering devices[5], and reflecting surfaces[6] have all been found with this technique. Though there have been advantageous designs for near-field focusing using the transformation method (and significant recent designs that do not use this method[7, 8]), the impact thus far on far-field imaging has been minimal. The reason for this is likely that straightforward application of the transformation method to free space, results in devices that affect no permanent change to fields outside the transformation media region. Since all practical devices are of finite size, manipulation of far-fields requires some extra considerations. One method to accomplish this involves the handling of discontinuities in the coordinate transformation[5]. Another method, the one employed here, is to transform a device, that already manipulates far-fields in some useful way, to improve or alter this functionality. Our starting point will be the Luneberg lens.

It is worth noting that the mathematical tools required for transformation design have been available for many decades[9]. What makes the method relevant now is the advancement of the field of metamaterials. Metamaterial technology allows one to implement the resulting complex material specifications which are often anisotropic and inhomogenous (with specific functional forms). To date, only one transformation based design has been built and tested[10], but I anticipate that advantageous transformation designs will provide additional incentive for further development of this enabling technology.

The Luneberg lens is far from being a new design[11]. It is sphere composed of an isotropic medium with refractive index functional form

$$n_L(r) = \sqrt{2 - \frac{r^2}{a^2}} \quad (1)$$

The index is unity on the surface of the bounding sphere of radius a , and $\sqrt{2}$ at its center. It possess quite remarkable focusing properties. In the geometric limit, it can focus parallel rays (i.e. those from an infinitely distant source) from any direction to a point on the opposite side of the sphere. Thus a spherical surface at infinity is aplanatic to the bounding spherical surface of the lens. Despite these remarkable and nearly ideal focusing properties, the Luneberg lens is rarely used. There are two reasons for this. One

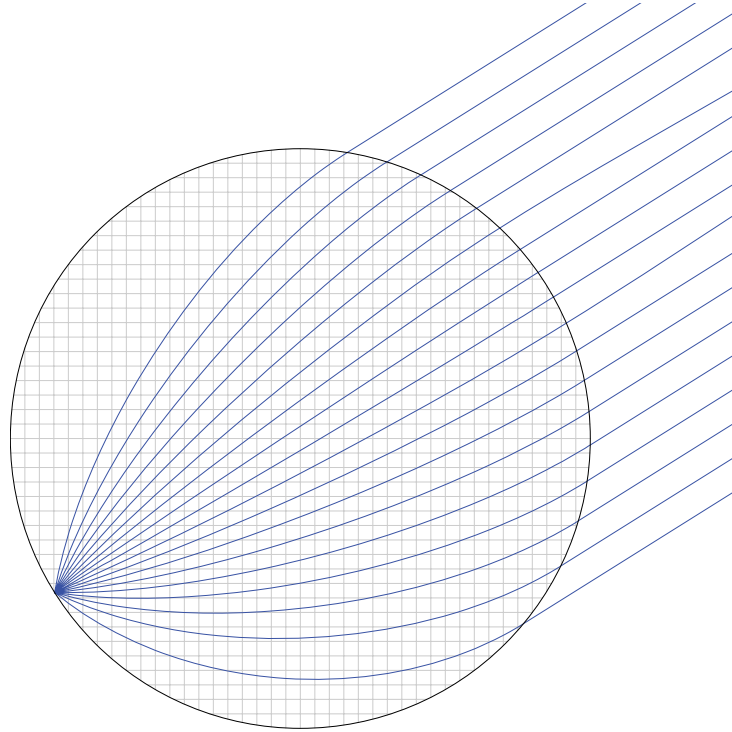


Fig. 1. The Luneberg lens. Paths of oblique rays (blue lines) from an infinitely distant source are focused onto the spherical surface of the lens opposite the source. The gray grid lines indicate the flat, Cartesian coordinates used in the untransformed domain.

is the need for precise control of the index profile which has large variations relative to those available with common glass GRIN technology. The second is that the image surface is spherical, requiring a spherical focal-plane detector-array for parallel image acquisition (i.e. acquisition without mechanical scanning). Planar focal-plane arrays or imaging chips represent a highly developed technology which leverages very mature planar lithographic processing techniques. This technology cannot be easily adapted for use with non-planar surfaces.

The essential idea presented in this article is to transform the Luneberg lens' spherical image surface into a planar one without compromising its aplanicity. The resulting transformation-modified Luneberg lens can have a pair of *planar* aplanatic surfaces, i.e. the lens produces a planar image with zero aberrations of all orders. Additionally, since the image can still form on the (now flat) back surface of the lens, the back focal length is zero as is the F-number defined from this focal length.

2 Transformation Design

As described elsewhere[12], the material properties that give the same electromagnetic behavior as a distorted space, are found from the transformation properties of the electromagnetic material property tensors. The electric permittivity, ϵ (or the magnetic

permeability , μ), transforms as a second rank tensor-density of unit weight[9].

$$\varepsilon^{i'j'} = \det \left(\Lambda^{i'}_i \right)^{-1} \Lambda^{i'}_i \Lambda^{j'}_j \varepsilon^{ij} \quad (2)$$

where $\Lambda^{i'}_i$ is the transformation operator. When the bases denoted by the indices i and i' are *coordinate* bases, the transformation operator derives quite simply as

$$\Lambda^{i'}_i = \frac{\partial x^{i'}}{\partial x^i} \quad (3)$$

from the functions describing the coordinate transformation

$$x^{i'} = x^{i'}(x^i) \quad (4)$$

However, it is common practice to write the desired transformation in terms of spherical or cylindrical coordinates and use the spherical *unit* basis (or the cylindrical *unit* basis) to describe the material properties. These *unit* bases are not directly derivable from their respective coordinate transformation functions[13]. Thus additional steps are needed to calculate the desired transformation operator. In this case the transformation operator can be written

$$\Lambda^{\hat{i}'}_{\hat{i}} = \Lambda^{\hat{i}'}_{i'} \Lambda^{i'}_i \Lambda^i_{\hat{i}} \quad (5)$$

where the hat on the indices denotes a *unit* basis. The right-most operator, $\Lambda^i_{\hat{i}}$, transforms geometric objects from a *unit* basis, \hat{i} , to a *coordinate* basis, i . The next operator, $\Lambda^{i'}_i$, transforms from one *coordinate* basis, i , to another, i' , (and can be found from the matrix of partials of the coordinate transformation functions (4)). The last (or left-most) operator, $\Lambda^{\hat{i}'}_{i'}$, transforms from the resulting *coordinate* basis, i' , back to a *unit* basis, \hat{i}' . To determine the transformation operators involving *unit* bases, one can use the relationship (valid for both coordinate and non-coordinate bases) between the basis vectors

$$\vec{e}_{i'} = \Lambda^{i'}_i \vec{e}_i \quad (6)$$

From this one finds

$$\vec{e}_{i'} \cdot \vec{e}_{\hat{j}'} = \Lambda^{\hat{j}'}_{i'} \delta_{\hat{i}\hat{j}'} \quad (7a)$$

$$\Lambda^i_{\hat{i}} \vec{e}_i \cdot \vec{e}_{\hat{j}} = \delta_{\hat{i}\hat{j}} \quad (7b)$$

In matrix form the Kronecker deltas will not be needed for consistency of contra- and covariant indices.

$$\left(\Lambda^{\hat{i}'}_{i'} \right) = \left(\vec{e}_{\hat{i}'} \cdot \vec{e}_{i'} \right) \quad (8a)$$

$$\left(\Lambda^i_{\hat{i}} \right) = \left(\vec{e}_{\hat{i}} \cdot \vec{e}_i \right)^{-1} \quad (8b)$$

For example, the functional relationship between Cartesian and spherical coordinates is

$$x = r \sin \theta \cos \phi \quad (9a)$$

$$y = r \sin \theta \sin \phi \quad (9b)$$

$$z = r \cos \theta \quad (9c)$$

so that using (3) the transformation operator from the spherical *coordinate* basis to the Cartesian basis is

$$\left(\Lambda^{i'}_{i'} \right) = \begin{pmatrix} \sin \theta \cos \phi & r \cos \theta \cos \phi & -r \sin \theta \sin \phi \\ \sin \theta \sin \phi & r \cos \theta \sin \phi & r \sin \theta \cos \phi \\ \cos \theta & -r \sin \theta & 0 \end{pmatrix} \quad (10)$$

and from (6) the spherical *coordinate* basis vectors are

$$\vec{e}_r = \sin \theta \cos \phi \vec{e}_x + \sin \theta \sin \phi \vec{e}_y + \cos \theta \vec{e}_z = \vec{e}_{\hat{r}} \quad (11a)$$

$$\vec{e}_\theta = r \cos \theta \cos \phi \vec{e}_x + r \cos \theta \sin \phi \vec{e}_y - r \sin \theta \vec{e}_z = r \vec{e}_{\hat{\theta}} \quad (11b)$$

$$\vec{e}_\phi = -r \sin \theta \sin \phi \vec{e}_x + r \sin \theta \cos \phi \vec{e}_y = r \sin \theta \vec{e}_{\hat{\phi}} \quad (11c)$$

and their relationship to the traditional unit basis is as shown on the right hand side. Then using (8) the relevant transformation matrices are given by

$$\left(\Lambda_{i'}^{\hat{i}'} \right) = \begin{pmatrix} 1 & 0 & 0 \\ 0 & r' & 0 \\ 0 & 0 & r' \sin \theta' \end{pmatrix} \quad (12a)$$

$$\left(\Lambda_{\hat{i}}^i \right) = \begin{pmatrix} 1 & 0 & 0 \\ 0 & \frac{1}{r} & 0 \\ 0 & 0 & \frac{1}{r \sin \theta} \end{pmatrix} \quad (12b)$$

Similarly, these transformation matrices for cylindrical coordinates are

$$\left(\Lambda_{i'}^{\hat{i}'} \right) = \begin{pmatrix} 1 & 0 & 0 \\ 0 & \rho' & 0 \\ 0 & 0 & 1 \end{pmatrix} \quad (13a)$$

$$\left(\Lambda_{\hat{i}}^i \right) = \begin{pmatrix} 1 & 0 & 0 \\ 0 & \frac{1}{\rho} & 0 \\ 0 & 0 & 1 \end{pmatrix} \quad (13b)$$

Note the consistent use of primed and un-primed coordinates. In (5), one first transforms from the un-primed *unit* to the *coordinate* basis, and last transforms from the primed *coordinate* to primed *unit* basis.

As an example of material property calculation, consider the spherical cloak coordinate transformation

$$r' = a + \frac{b-a}{b} r \quad (14a)$$

$$\theta' = \theta \quad (14b)$$

$$\phi' = \phi \quad (14c)$$

for which the transformation operator between the *coordinate* bases is

$$\left(\Lambda_{i'}^{\hat{i}'} \right) = \begin{pmatrix} \frac{b-a}{b} & 0 & 0 \\ 0 & 1 & 0 \\ 0 & 0 & 1 \end{pmatrix} \quad (15)$$

and the total transformation operator is

$$\left(\Lambda_{\hat{i}}^{\hat{i}'} \right) = \begin{pmatrix} \frac{b-a}{b} & 0 & 0 \\ 0 & \frac{r'}{r} & 0 \\ 0 & 0 & \frac{r' \sin \theta'}{r \sin \theta} \end{pmatrix} = \begin{pmatrix} \frac{b-a}{b} & 0 & 0 \\ 0 & \frac{r'}{r} & 0 \\ 0 & 0 & \frac{r'}{r} \end{pmatrix} \quad (16)$$

From (2), and using free space as the initial material (which is represented by the identity matrix in the spherical *unit* basis, but *not* in the spherical *coordinate* basis), and expressing solely in terms of the primed coordinates, one obtains the well known result[1].

$$\left(\hat{\varepsilon}^{\hat{i}'} \hat{j}' \right) = \frac{b}{b-a} \begin{pmatrix} \frac{(r'-a)^2}{r'^2} & 0 & 0 \\ 0 & 1 & 0 \\ 0 & 0 & 1 \end{pmatrix} \quad (17)$$

3 Transforming the Luneberg lens

3.1 Simple Case

There are an infinite number of ways to flatten the image surface of a Luneberg lens. Perhaps the simplest is

$$\rho' = \rho \quad (18a)$$

$$\phi' = \phi \quad (18b)$$

$$z' = \frac{1}{2}(z + z_a) \quad (18c)$$

written in standard cylindrical coordinates. These transformation functions apply on the domain of the un-flattened Luneberg sphere, $\sqrt{\rho^2 + z^2} < a$, where a is the radius of the sphere, and z_a is defined by

$$z_a = \sqrt{a^2 - \rho^2} \quad (19)$$

No attempt is made to maintain continuity of the coordinate transformation at $z' = 0$ since it is assumed that an opaque focal-plane array-detector will be located at that position, and the fields will not penetrate beyond that point. The coordinate transformation matrix is given by

$$\left(\Lambda_{i'}^{i'} \right) = \begin{pmatrix} 1 & 0 & 0 \\ 0 & 1 & 0 \\ -\frac{\rho}{2z_a} & 0 & \frac{1}{2} \end{pmatrix} = \left(\Lambda_{\widehat{i}}^{\widehat{i}} \right) \quad (20)$$

and in this case, where the cylindrical radial coordinate is un-transformed, the total transformation matrix is the same expression. Using (2) and combining with (13) the material properties are

$$\left(\varepsilon^{\widehat{i}'\widehat{j}'} \right) = \left(\mu^{\widehat{i}'\widehat{j}'} \right) = n_L(r) \begin{pmatrix} 2 & 0 & -\frac{\rho'}{z_a} \\ 0 & 2 & 0 \\ -\frac{\rho'}{z_a} & 0 & \frac{1}{2} \left(1 + \frac{\rho'^2}{z_a^2} \right) \end{pmatrix} \quad (21)$$

where I have assumed the Luneberg index profile is comprised of equal values of the permittivity and the permeability

$$\varepsilon^{\widehat{i}\widehat{j}} = \mu^{\widehat{i}\widehat{j}} = n_L(r) \delta^{\widehat{i}\widehat{j}} \quad (22)$$

The un-primed spherical radial coordinate, r , is expressed in terms of the primed cylindrical coordinates as

$$r = \sqrt{\rho^2 + z^2} = \sqrt{\rho'^2 + (2z' - z_a)^2} = \sqrt{\rho'^2 + \left(2z' - \sqrt{a^2 - \rho'^2} \right)^2} \quad (23)$$

For implementation using metamaterials, it is helpful to express (21) in a principle (i.e. diagonalizing) basis. An orthogonal diagonalizing basis can always be found since (2) always provides Hermitian matrices. Using standard techniques one finds

$$\left(\varepsilon^{\widehat{i}''\widehat{j}''} \right) = \left(\mu^{\widehat{i}''\widehat{j}''} \right) = n_L(r) \begin{pmatrix} 1/\eta & 0 & 0 \\ 0 & 2 & 0 \\ 0 & 0 & \eta \end{pmatrix} \quad (24)$$

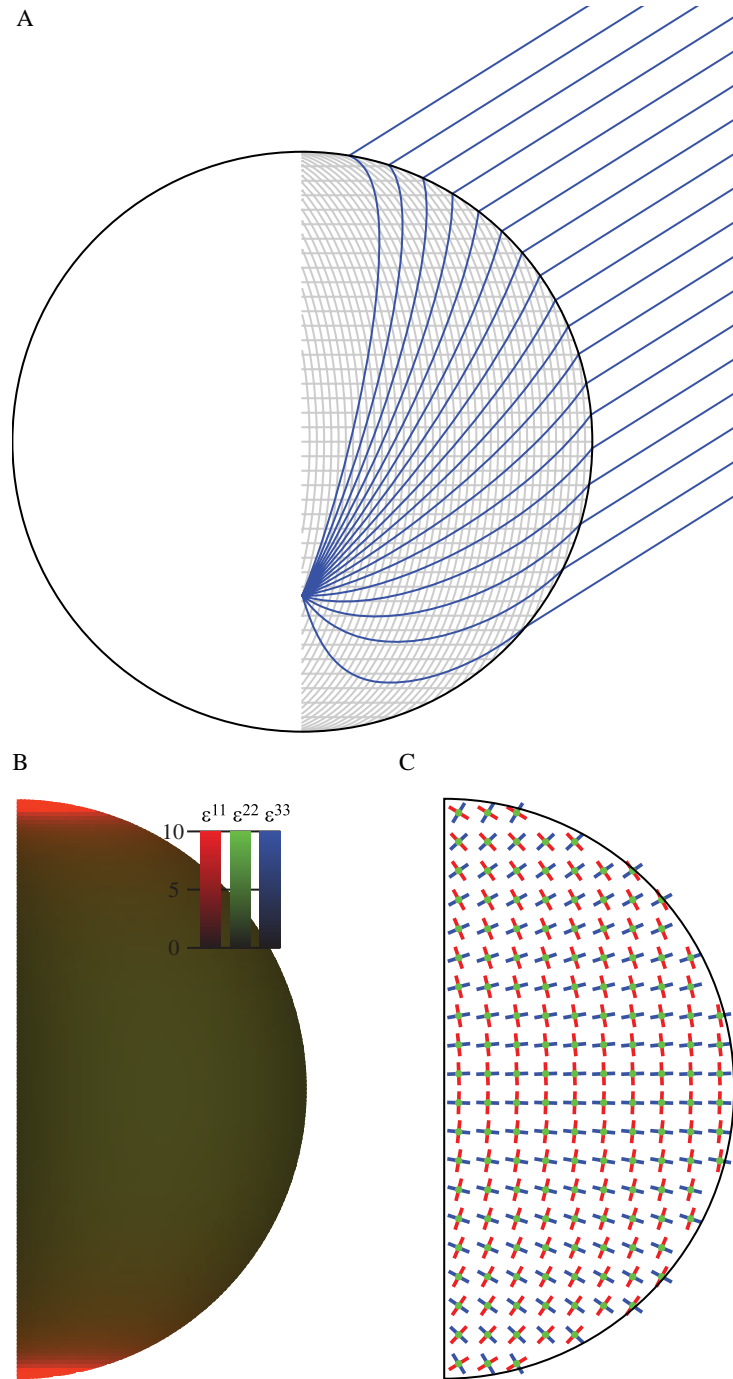


Fig. 2. Simple transformation of Luneberg lens, where the cylindrical radial coordinate is untransformed. (A) Paths of oblique rays (blue lines) from a distant source are focused onto the flat image plane. The grid (gray lines) is the same as that shown in Fig. 1, but transformed according to (18). (B) Principle elements of the material property tensors represented in the three color channels, red, green and blue. Isotropic media would be represented by gray scale regions where the three color channels would have equal values. The red channel (which can be associated with the cylindrical radial component in the untransformed coordinate system) saturates at the lens edge since that material component is divergent there. (C) The three principle directions of the material property tensors. The green channel direction is out of the page and represents the ϕ component which is untransformed.

where

$$\eta = \frac{5a^2 - 4\rho'^2 - a\sqrt{9a^2 - 8\rho'^2}}{4(a^2 - \rho'^2)} \quad (25)$$

The function η ranges from plus one half to zero as ρ' ranges from zero to a . This of course means that the first component of the material property tensors, $\varepsilon^{\hat{1}''\hat{1}''} = \mu^{\hat{1}''\hat{1}''}$, diverges at the circumference of the lens. However, it does so sharply and near the boundary, so that the most of the aperture can be correctly implemented with material property values less than ten. The diagonal basis vectors are

$$\vec{e}_{\hat{1}''} \rightarrow (-1/\gamma, 0, 1) / \sqrt{1/\gamma^2 + 1} \quad (26a)$$

$$\vec{e}_{\hat{2}''} \rightarrow (0, 1, 0) \quad (26b)$$

$$\vec{e}_{\hat{3}''} \rightarrow (\gamma, 0, 1) / \sqrt{\gamma^2 + 1} \quad (26c)$$

where

$$\gamma = \frac{-3a^2 + 4\rho'^2 + a\sqrt{9a^2 - 8\rho'^2}}{4\rho'\sqrt{a^2 - \rho'^2}} \quad (27)$$

3.2 Distortion Free

While the previous transformation results in a lens that does not introduce any defocusing geometric aberrations, the lens does contribute non-lossy distortions such as "barrel" distortion. One can in principle correct these types of distortions in post processing of the image file, but this results in sensor pixel data being distributed in a non-uniform way over the corrected image, and in any case, the post processing transformation can be built into the lens, resulting in a completely geometric aberration free lens. In removing these distortions, several other changes are introduced.

Unlike the lens described above, which has a field-of-view approaching 180 degrees (i.e. 2π steradians of solid angle), the field-of-view must be restricted. For a zero F-number lens, the field stop and the aperture stop are the same, and restricted to be less than (or equal to) the lens diameter, which is finite. Clearly, an infinite object (filling a 180 degree field-of-view) cannot be mapped into a finite field stop without distortion.

The transformation (and all those like it with fields of view less than 180 degrees) will result in material properties that are everywhere finite.

If the field-of-view is set to less than 90 degrees, the lens will have constant aperture of area, πa^2 , for all incident angles within the field-of-view. In contrast, the lens described above presents an aperture of area πa^2 for direct incidence, but only half that for edge-on incidence. All traditional lenses that use only partial spherical surfaces also have aperture reduction off axis. Constant aperture, and thus constant and undiminished light collection capability is a useful feature.

The proposed distortion free transformation is

$$\rho' = \frac{1}{2} \left(1 - \frac{z}{z_a} \right) \frac{a \cos \psi}{z_a} \rho + \frac{1}{2} \left(1 + \frac{z}{z_a} \right) \rho \quad (28a)$$

$$\phi' = \phi \quad (28b)$$

$$z' = \frac{1}{2} \left(1 + \frac{a \cos \psi}{z_a} \right) z + \frac{1}{2} \left(1 - \frac{a \cos \psi}{z_a} \right) z_a \quad (28c)$$

where ψ is the half angle of the field-of-view cone. These functions apply on the domain where $\rho < a \sin \psi$. (The identity transformation is used elsewhere in the spherical domain $\sqrt{\rho^2 + z^2} < a$.) This transformation remaps a portion of the spherical surface onto a flat truncation of the sphere in such a way that the resulting lens focuses flat object planes

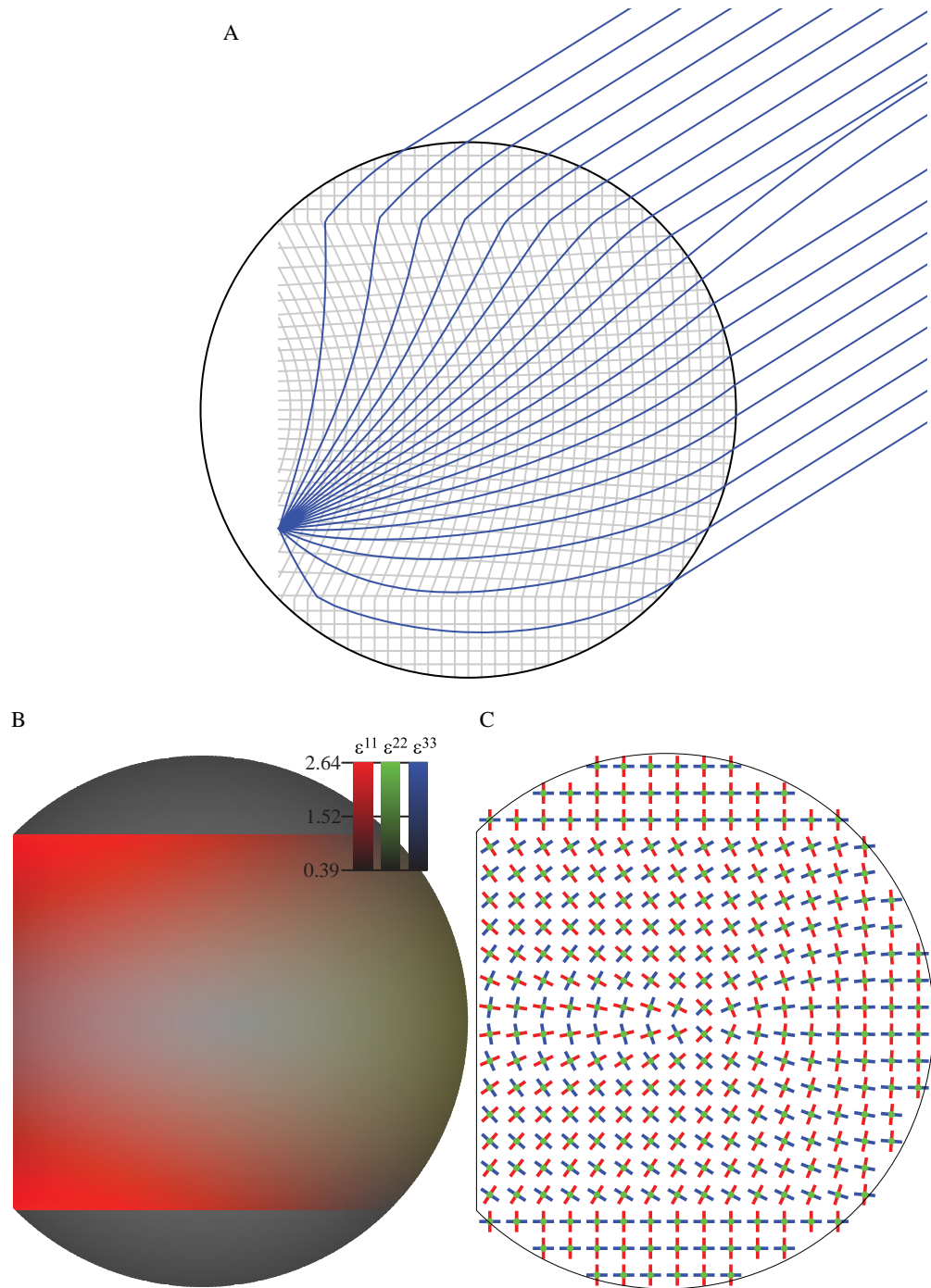


Fig. 3. Distortion free transformation of Luneberg lens with 90 degree field of view (i.e. $\psi = \pi/4$). (A) Paths of oblique rays (blue lines) from a distant source are focused onto the flat image plane. The grid (gray lines) is the same as that shown in Fig. 1, but transformed according to (28). (B) Principle elements of the material property tensors represented in the three color channels, red, green and blue. Isotropic media are represented by gray scale regions where the three color channels have equal values. There is no saturation in this figure. The principle values are everywhere between 0.39 and 2.64. (C) The three principle directions of the material property tensors. The green channel direction is out of the page and represents the ϕ component which is untransformed.

without distortion onto the resulting flat image plane. This image plane remapping can be found by setting $z = -z_a$ (i.e. the back surface of the sphere) in (28a) yielding

$$\rho' = \frac{a \cos \psi}{z_a} \rho \quad (29)$$

where ρ is the cylindrical radius of a point on the spherical section and ρ' is the cylindrical radius of the corresponding point on the truncation flat. The remaining details of the transformation are set by requiring it to be the identity when $z = z_a$ (i.e. the front surface of the sphere), and a linear combination of the the identity and (29) in the intervening volume.

There is no point (nor sufficient space) to show the calculation leading to the diagonal material property tensors for this transformation. In any case, analytical inversion of (28) does not appear to be feasible. As this is required to find the material properties in terms of the coordinates applicable to material space, a complete analytical expression may not be possible. To generate the data for Fig. (3), numerical inversion was used. Fig. (3) shows the ray trajectories and material properties for a lens with $\psi = \pi/4$ (i.e. a field-of-view of 90 degrees).

4 Conclusion

With its aplanatic surfaces the Luneberg lens is an excellent starting point for transformation design enhancements. Enabling the use of high performance off-the-shelf detector arrays, transforming to a flat image surface makes the Luneberg lens much more practical. Such a lens, with its complete lack of image aberration, zero F-number and constant aperture is attractive for any application where a single element, high performance and extremely compact far-field imaging system is desired. However, even with recent advances in the field of metamaterials, it will be a challenge to implement. And like all metamaterial devices, will be subject to limited bandwidth and non-negligible absorption. However, perhaps this and other advantageous transformation designs will help to drive progress in these areas.

References and links

1. J.B. Pendry, D. Schurig, and D.R. Smith. Controlling electromagnetic fields. *Science*, 312(5781):1780 – 2, 2006/06/23.
2. Marco Rahm, David Schurig, Daniel A. Roberts, Steven A. Cummer, David R. Smith, and John B. Pendry. Design of electromagnetic cloaks and concentrators using form-invariant coordinate transformations of Maxwell’s equations. *PHOTONICS AND NANOSTRUCTURES-FUNDAMENTALS AND APPLICATIONS*, 6(1):87–95, APR 2008.
3. Steven A. Cummer, Bogdan-Ioan Popa, David Schurig, David R. Smith, John Pendry, Marco Rahm, and Anthony Starr. Scattering theory derivation of a 3D acoustic cloaking shell. *PHYSICAL REVIEW LETTERS*, 1(2), JAN 18 2008.
4. D. Schurig, J.B. Pendry, and Smith D.R. Planar focusing antenna design by using coordinate transformation technology. *Optics Express*, 15(22):14772–14782, 2007.
5. Marco Rahm, Steven A. Cummer, David Schurig, John B. Pendry, and David R. Smith. Optical design of reflectionless complex media by finite embedded coordinate transformations. *PHYSICAL REVIEW LETTERS*, 1(6), FEB 15 2008.
6. Fanmin Kong, Bae-Ian Wu, Jin Au Kong, Jiangtao Huangfu, Sheng Xi, and Hongsheng Chen. Planar focusing antenna design by using coordinate transformation technology. *Applied Physics Letters*, 91(25):253509 –, 2007. Metamaterials;Planar antennas;Planar focusing antennas;
7. J.B. Pendry. Negative refraction makes a perfect lens. *Physical Review Letters*, 85(18):3966 – 9, 2000/10/30.
8. Z. Jacob, L.V. Alekseyev, and E. Narimanov. Optical hyperlens: far-field imaging beyond the diffraction limit. *Optics Express*, 14(18), Sept. 2006.
9. E.J. Post. *Formal structure of electromagnetics*. Wiley, 1962.
10. D. Schurig, J.J. Mock, B.J. Justice, S.A. Cummer, J.B. Pendry, A.F. Starr, and D.R. Smith. Metamaterial electromagnetic cloak at microwave frequencies. *Science*, 314(5801):977 – 80, 2006/11/10.
11. Max Born and Emil Wolf. *Principles of Optics*. Pergamon Press, Oxford, sixth edition, 1993.

12. D. Schurig, J.B. Pendry, and D.R. Smith. Calculation of material properties and ray tracing in transformation media. *Optics Express*, 14(21), 2006/10/.
 13. Schutz B.F. *A first course in general relativity*. Cambridge University Press, 1985.
-